SPARC-BD-07/005
15 November 2007

COHERENT EMISSION FROM AN ELECTRON BUNCH WITH A COMB STRUCTURE

M. Castellano, E. Chiadroni *(INFN/LNF)*

Abstract

In this note we study the Coherent Radiation emission by an electron bunch with a comb structure. The radiation can be used as a source for dedicated users or as a diagnostic tool for the bunch itself.

1. INTRODUCTION

In the frame of the development of the SPARC photoinjector, the possibility of producing, directly from the source, an electron bunch with a longitudinal density modulation is considered [1, 2]. Such a "comb" structure can be useful for several applications, from increasing the local peak current for FEL production to the generation of synchronized pump-and-probe sequences.
In order to clarify some possible use and/or the diagnostics of this kind of bunch structure, in this note we will illustrate the coherent spectrum of radiation emitted by a "comb" electron bunch. The results presented here are applicable to any radiation process in which the bunch structure is "frozen" during the emission process, and in particular there is no interaction between particle and radiation.
This is the case of Transition Radiation and Diffraction Radiation, in which the emission is a surface phenomenon and thus almost instantaneous. But also Cherenkov Radiation, Synchrotron Radiation and Spontaneous Radiation in undulators can be treated in the same way if the electron distribution inside the bunch can be considered constant during the emission.
If $\frac{dI_{sp}}{d\omega\, d\Omega}$ is the distribution of the radiation intensity emitted by a single particle, supposed concentrated in a narrow cone in the forward direction, the emission from a bunch of longitudinal profile g(x) is normally written as

$$\frac{dI}{d\omega\, d\Omega} = \frac{dI_{sp}}{d\omega\, d\Omega}\left[N + N(N-1)F(\omega)\right] \tag{1}$$

in which N is the total number of particle in the bunch and F(ω) the "longitudinal form factor" of the bunch itself defined as

$$F(\omega) = \left| \int_{-\infty}^{\infty} g(x) e^{-i\frac{\omega}{c}x}\, dx \right|^2 \tag{2}$$

With a typical electron bunch produced by a photoinjector RF gun, containing a number of particles of the order of 10^9, the coherent part of the spectrum is strongly enhanced by its N^2 dependence, and results the more interesting both as possible source of FIR radiation and as diagnostic tool of the bunch structure.
Ignoring for the moment the absolute intensity value, and also the possible frequency dependence of the single particle emission, let us look more in detail on the behavior of the form factor F(ω) in the case of a comb longitudinal structure, that is a succession of narrow pulses whose separation is of the order or larger than their width.
Without losing too much generality, to illustrate some feature of the coherent spectrum emitted by this kind of structure we can assume a succession of gaussian pulses.
Let's start with a 3 mm pulse subdivided into 11 subpulses of 50 μm width (sigma) and separated by 300 μm, as shown in Fig. 1.
In Fig. 2 is presented the form factor of a single subpulse, while in Fig 3 the form factor of the whole comb pulse is superimposed to the previous one.

All the form factors are normalized to 1, so that to obtain the coherent intensity, the form factors must be multiplied by N^2, with N the total number of particle involved in the distribution considered.
From Figs.2 and 3 it is evident that the spectrum of the narrower single subpulse is the larger one, and that a regular succession of similar pulses produce a strong suppression of all the frequencies apart the one corresponding to the succession itself, reaching at most the value of the single subpulse case. It must be noted that in order to obtain the same radiation intensity at this frequency, in the case of a single pulse all the electrons N must be concentrated in the single pulse itself, in order to have the same N^2 coefficient. The width of this line depends on the number of pulses that constitutes the comb.

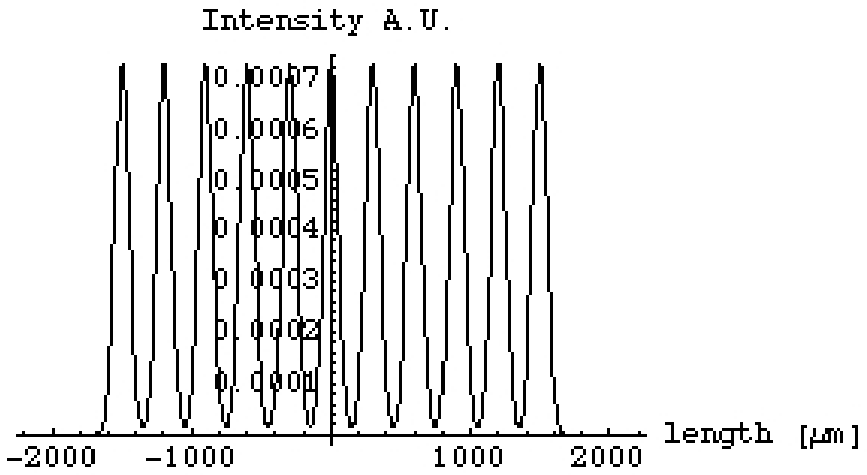

Fig. 1 – Comb pulse composed by 11 subpulses of σ=50 μm and separation 300 μm

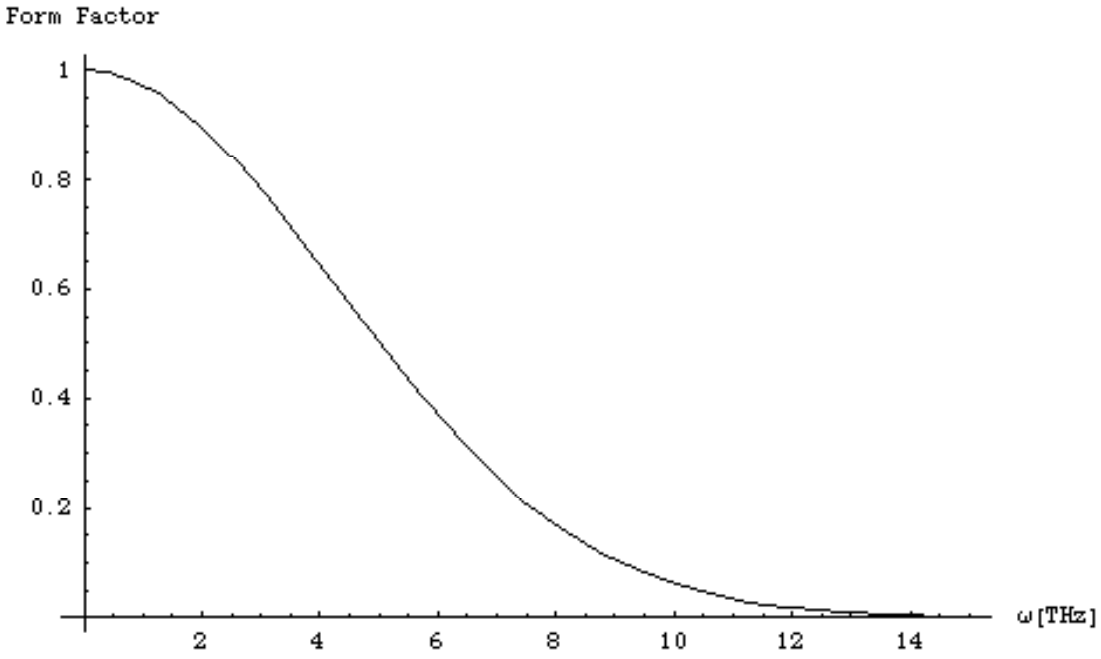

Fig. 2 – Form Factor of a single subpulse

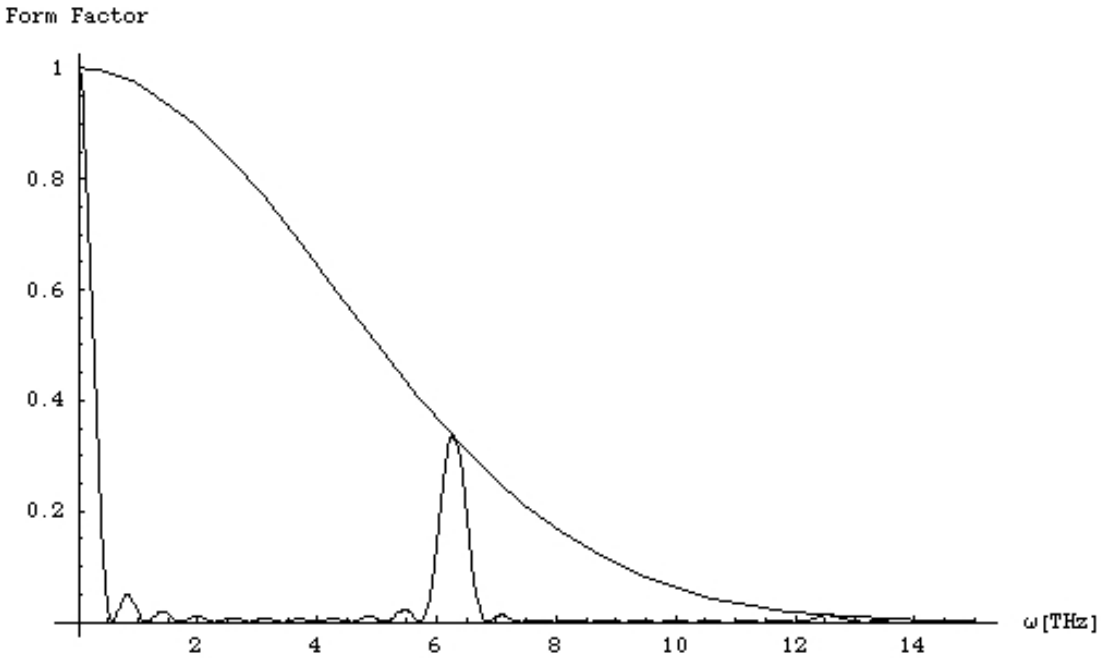

Fig. 3 – Superposition of the Form Factor of a single subpulse and that of the whole comb structure

At low frequencies, the comb structure has the same spectrum as a square pulse with the same width and rise/fall time, as is shown in Figs. 4 and 5. The only difference is the absence of the frequency line originated by the repetition of the comb subpulses.

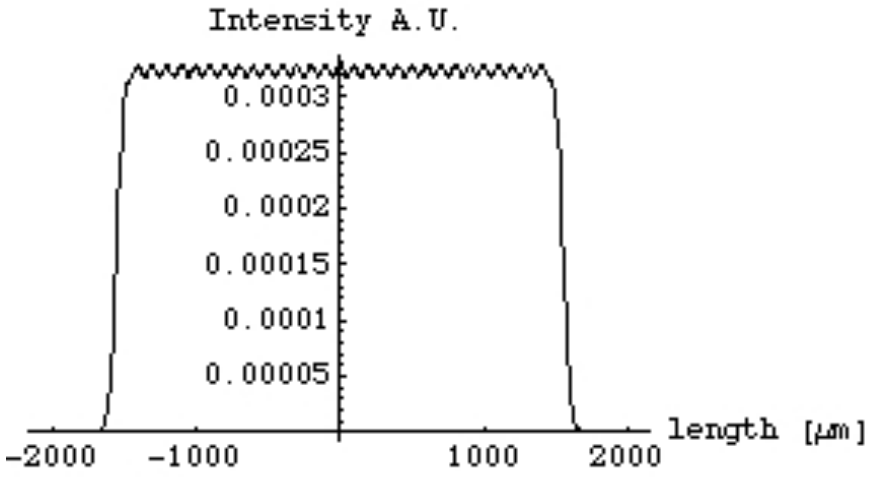

Fig. 4 – Square pulse with same width and rise/fall time of the comb structure

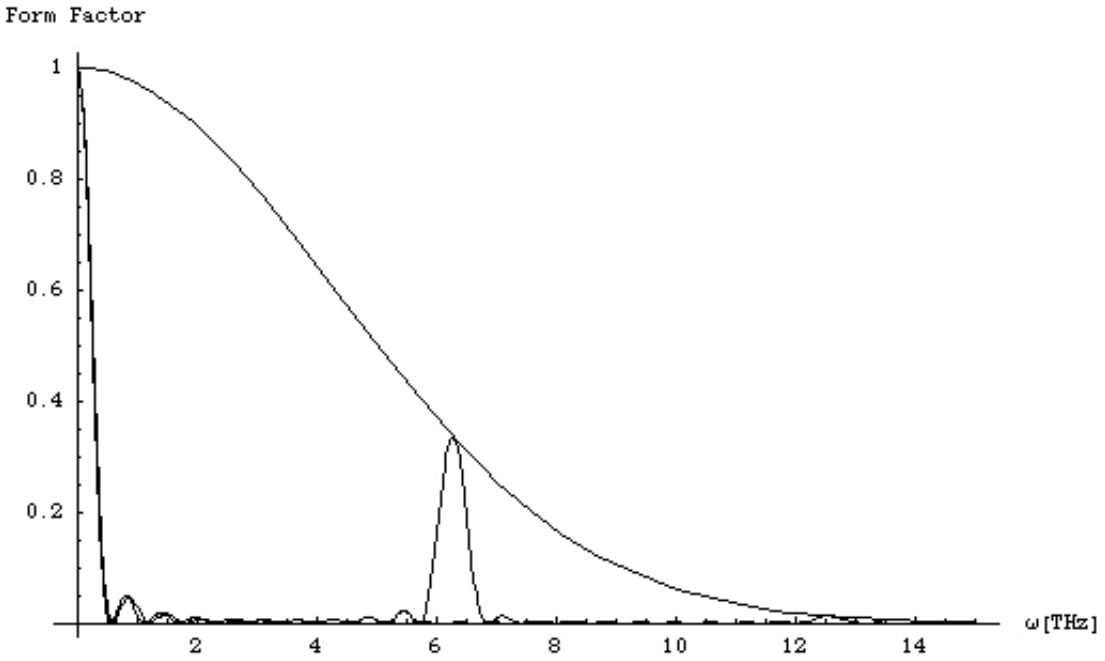

Fig. 5 – Superposition of all the Form Factors

If the width of the micropulses that constitutes the comb is reduced, the single pulse spectrum becomes larger, and more harmonics of the micropulse repetition frequency appears in the comb spectrum, but always limited by the single pulse spectrum, as is shown in Fig. 6.

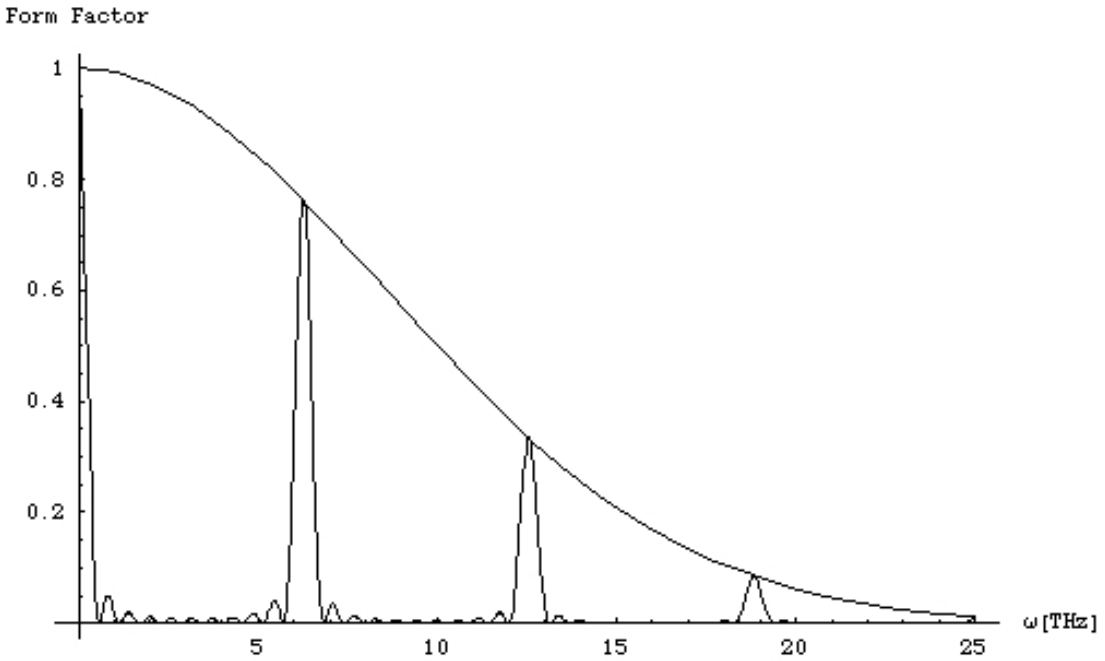

Fig. 6 – Spectrum of a comb with subpulses of 25 μm sigma and the single pulse spectrum

If, on the contrary, the micropulse width is increased, the modulation depth is reduced, as shown in Fig. 7 in which the sigma of the micropulses is of 100 μm, and

in the spectrum the intensity of the comb frequency is strongly suppressed (see Fig. 8).

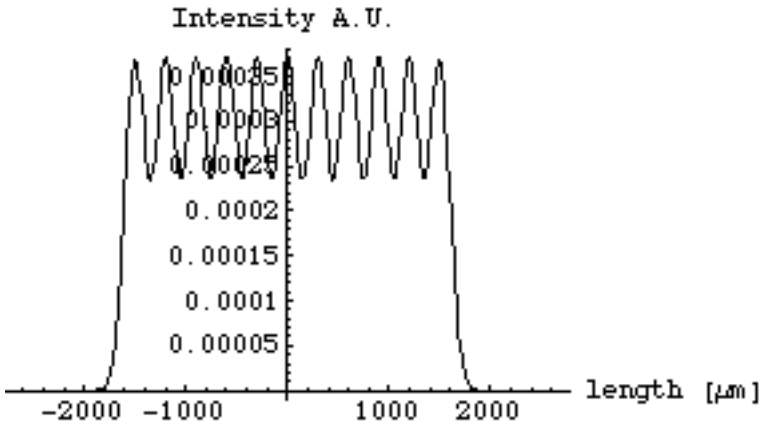

Fig. 7 – Pulse shape with a microbunch width of 100 μm

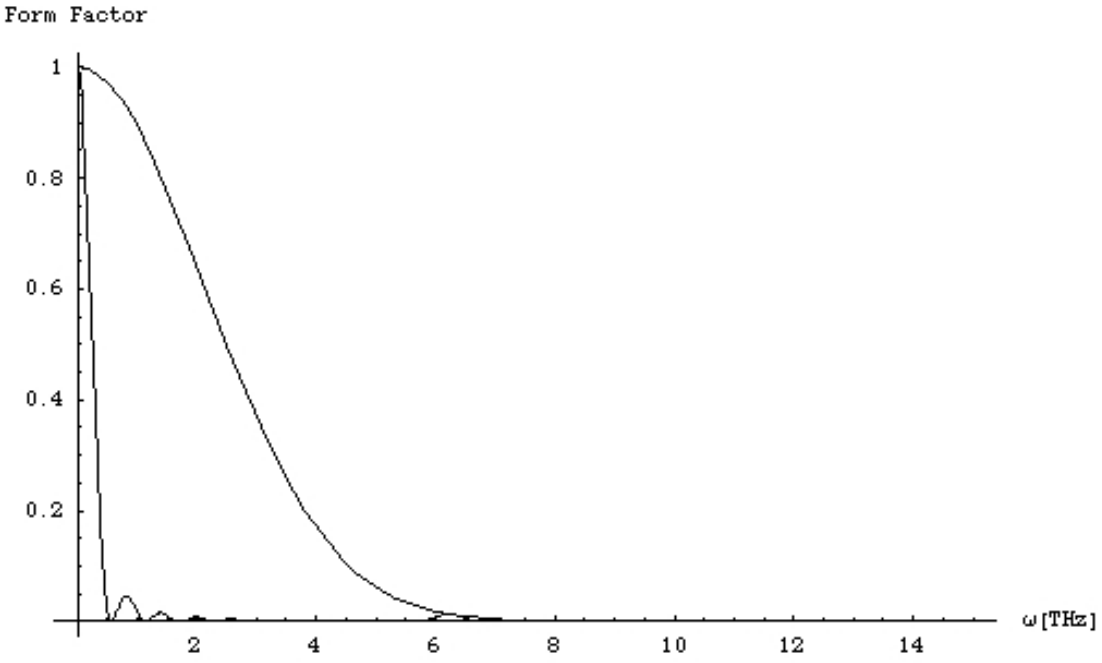

Fig. 8 – Spectrum of a single pulse with a 100 μm width and of the corresponding comb structure

These few examples show a possible use of a comb structure in the production of a strong coherent radiation at the frequency of the comb itself. Indeed at this frequency, and its higher harmonics, the intensity emitted by the comb is the same emitted by a single micropulse in which all the electrons of the comb are compressed. On the other hand, the modulation depth, i.e. the width of the single micropulse compared with their distance, will determine the overall spectrum, making more o less intense these lines.

A second possible application of a comb bunch is the generation of two narrow micropulses perfectly synchronized each other but with a variable time delay, to perform pump-and-probe measurements.

In this case, the coherent radiation can be used as a diagnostic tool. Although the RF deflector is the ideal instrument for this kind of measurement, the spectral content of the coherent radiation, measured with some kind of interferometer, can be complementary, and also superior for microbunches separation of the order of 200 μm or less.
To give an idea of what kind of coherent spectrum one can expect from two microbunches with variable spacing, in Fig. 9 is shown the comb bunch and its spectrum when two microbunches of sigma 300 μm start to separate from each other.

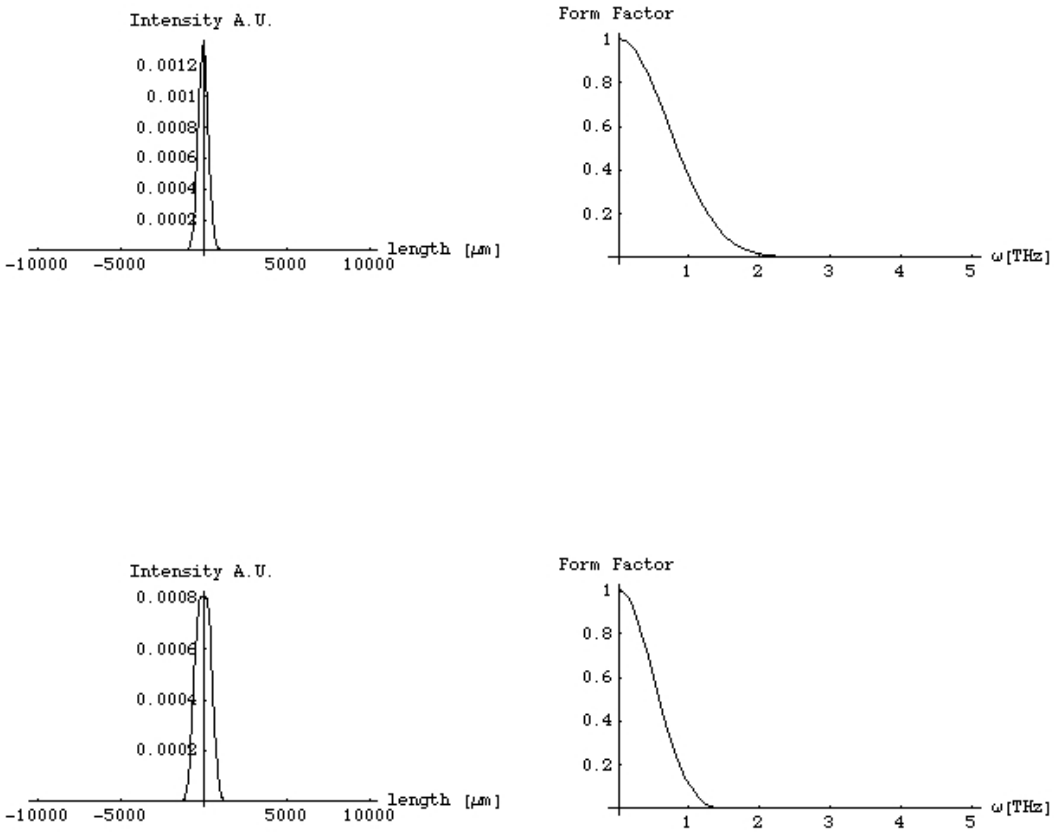

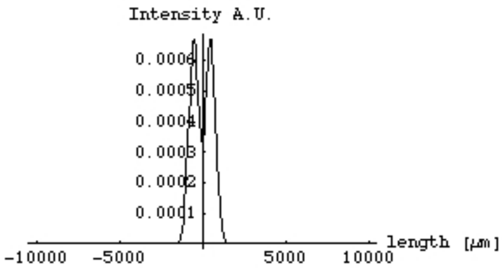
Intensity A.U.
0.0006
0.0005
0.0004
0.0003
0.0002
0.0001
-10000
-5000
5000
10000
length [μm]

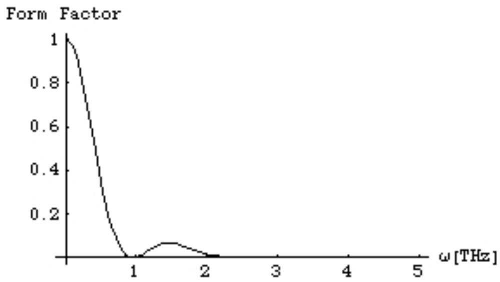
Form Factor
1
0.8
0.6
0.4
0.2
1
2
3
4
5
ω[THz]

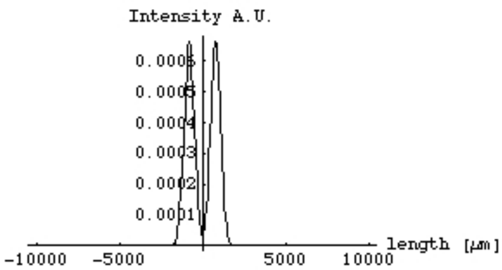
Intensity A.U.
0.0004
0.0003
0.0002
0.0001
-10000
-5000
5000
10000
length [μm]

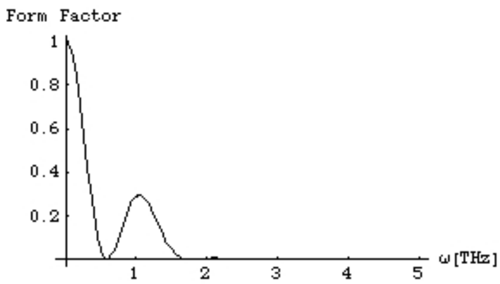
Form Factor
1
0.8
0.6
0.4
0.2
1
2
3
4
5
ω[THz]

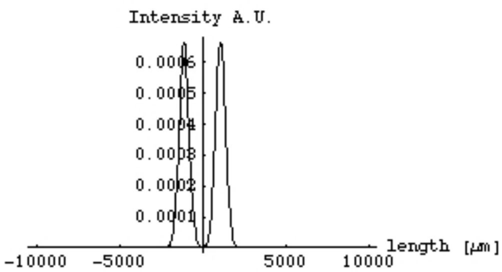
Intensity A.U.
0.0006
0.0005
0.0004
0.0003
0.0002
0.0001
-10000
-5000
5000
10000
length [μm]

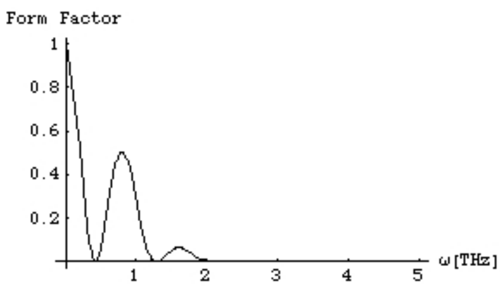
Form Factor
1
0.8
0.6
0.4
0.2
1
2
3
4
5
ω[THz]

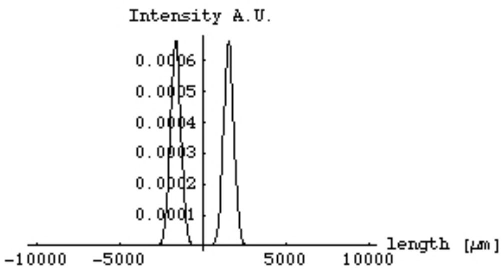
Intensity A.U.
0.0006
0.0005
0.0004
0.0003
0.0002
0.0001
-10000
-5000
5000
10000
length [μm]

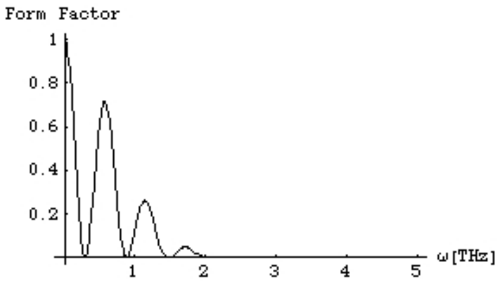
Form Factor
1
0.8
0.6
0.4
0.2
1
2
3
4
5
ω [THz]

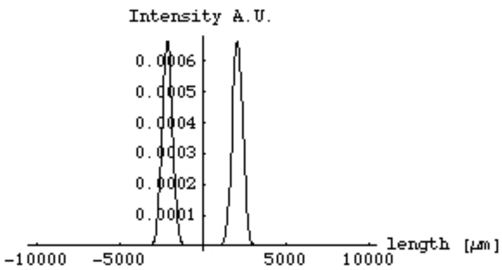
Intensity A.U.
0.0006
0.0005
0.0004
0.0003
0.0002
0.0001
-10000
-5000
5000
10000
length [μm]

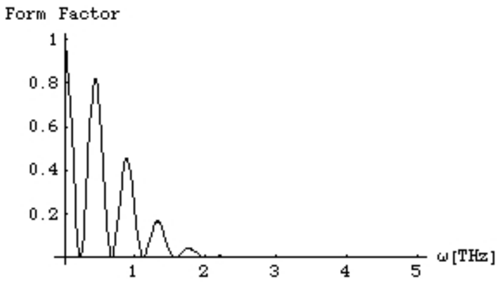
Form Factor
1
0.8
0.6
0.4
0.2
1
2
3
4
5
ω [THz]

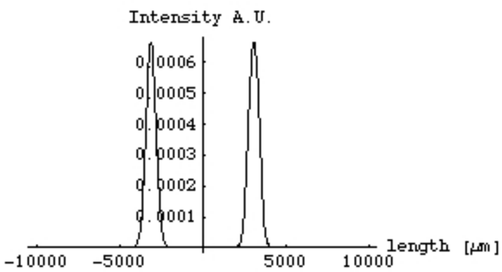
Intensity A.U.
0.0006
0.0005
0.0004
0.0003
0.0002
0.0001
-10000
-5000
5000
10000
length [μm]

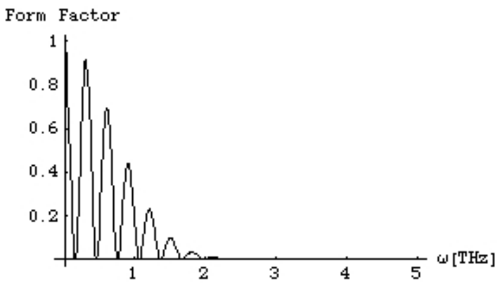
Form Factor
1
0.8
0.6
0.4
0.2
1
2
3
4
5
ω [THz]

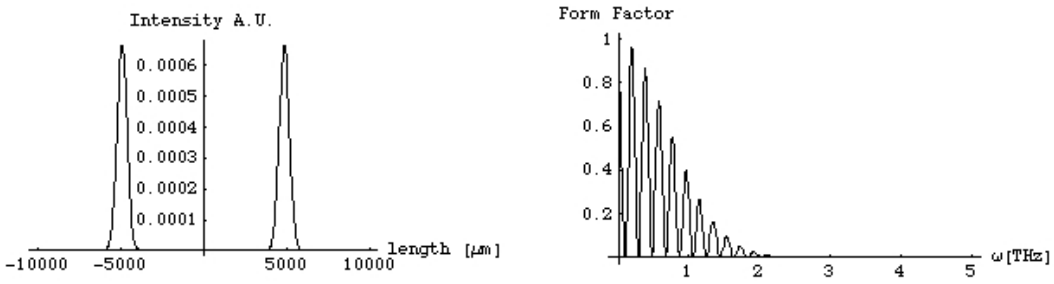

Fig. 9 – The Form Factor of two separating microbunches of sigma 300 μm

It is evident that when the two microbunches starts to separate, the single pulse spectrum is reduced, and oscillations appears. Always contained in the single pulse spectrum envelope. As the distance between the two pulses becomes much higher than their width, the oscillations are so narrow that any integration on the finite bandwidth of the detector, and on any finite solid angle, gives an effective form factors equal to one half of that of the single pulse, corresponding to the two sources, of half the number of the total electrons each, to contribute independently as individual and incoherent sources.

3. EXPERIMENTAL CONSIDERATIONS

Experimentally, the form factor of this kind of electron distribution can be retrieved by means of Fourier transform spectroscopy, based on the fact that the interference pattern from a two beams interferometer is the Fourier transform of the radiation passing through it. Any kind of source which does not change the electron distribution can be used, transition radiation, edge radiation from a dipole, undulator radiation.
In particular, for millimiter and sub-millimiter radiation a Martin-Puplett interferometer is normally considered. Compared to the better known Michelson interferometer, the beam splitter is replaced by a polarizing grid, whose wires are at 45° with respect to the horizontal plane when view along the beam axis. The grid reflects the field with polarization parallel to the wires and transmits the orthogonal one. The frequency range over which this effect is present depends on wires spacing and thickness. Furthermore, the plane mirrors are replaced by roof mirrors which rotate the polarization of the incident field upon reflection. A simplified sketch of a Martin-Puplett interferometer is shown in Fig.10.

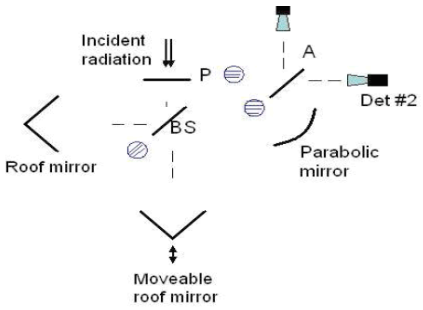

Fig. 10 – Schematic view of a Martin-Puplett interferometer

Since the beam divider has wires placed at 45°, the incident electric field will be split into a reflected field $\vec{E}_r$ and a transmitted field $\vec{E}_t$ such that

$$\begin{aligned}\vec{E}_t(t) &= \tfrac{E_0}{\sqrt{2}}\sin(\omega t)\frac{\hat{u}_h + \hat{u}_v}{\sqrt{2}} \\ \vec{E}_r(t) &= \tfrac{E_0}{\sqrt{2}}\sin(\omega t)\frac{\hat{u}_h - \hat{u}_v}{\sqrt{2}}\end{aligned} \tag{3}$$

with E_0 the peak electric field and $\hat{u}_h, \hat{u}_v$ the horizontal and vertical unit vectors.

At the roof mirrors, the $\hat{u}_h + \hat{u}_v$ component will be reflected with its plane of polarization altered to $\hat{u}_h - \hat{u}_v$ and similarly the $\hat{u}_h - \hat{u}_v$ component will change into $\hat{u}_h + \hat{u}_v$ upon reflection. As the movable mirror is moved, producing a path length difference, $2\Delta x$, between the two beams, the electric field components will go back to the polarizing beam splitter differing by a phase factor $\tau = \dfrac{2\Delta x}{c}$, as given by

$$\begin{aligned}\vec{E}_t'(t) &= \vec{E}_t(t-\tau) = \frac{E_0}{\sqrt{2}}\sin[\omega(t-\tau)]\frac{\hat{u}_h + \hat{u}_v}{\sqrt{2}} \\ \vec{E}_r'(t) &= \vec{E}_r(t) = \frac{E_0}{\sqrt{2}}\sin(\omega t)\frac{\hat{u}_h - \hat{u}_v}{\sqrt{2}}\end{aligned} \tag{4}$$

The reflected and transmitted components recombine to produce a total field, $\vec{E}_f = \vec{E}_r' + \vec{E}_t'$, at the analyzer which can be written by using trigonometric addition formulas as

$$\vec{E}_f(t) = E_0\left[\sin\left[\omega\left(t-\frac{\tau}{2}\right)\right]\cos\left(\frac{\omega\tau}{2}\right)\hat{u}_h + \sin\left(\frac{\omega\tau}{2}\right)\cos\left[\omega\left(t-\frac{\tau}{2}\right)\right]\hat{u}_v\right] \tag{5}$$

The horizontal and vertical components are 90° out of phase and the amplitudes depend on the phase difference, $\omega\tau$, resulting in an elliptically polarized radiation.

Assuming a source with an arbitrary intensity distribution, $\dfrac{dI}{d\omega\, d\Omega} = I(\omega)$, the intensity of the recombined radiation at the detectors can be written as

$$V_{h,v} \propto \int_{-\infty}^{\infty}\left(\vec{E}_f \cdot \hat{u}_{h,v}\right)^2 dt \tag{6}$$

which becomes

$$V_{h,v}(\tau) \propto \int_0^\infty I(\omega) \begin{Bmatrix} \cos^2\left(\frac{\omega\tau}{2}\right) \\ \sin^2\left(\frac{\omega\tau}{2}\right) \end{Bmatrix} d\omega \tag{7}$$

The normalized difference interferogram then can be written as

$$\delta(\tau) = \frac{V_h(\tau) - V_v(\tau)}{V_h(\tau) + V_v(\tau)} = \frac{\int_0^\infty I(\omega)\cos(\omega\tau)d\omega}{\int_0^\infty I(\omega)d\omega} \tag{8}$$

which corresponds to the Fourier transform of the radiation spectrum and is the measured quantity. The frequency spectrum of the incident radiation pulse can then be obtained by inverse Fourier transforming $\delta(\tau)$. From Eq.1 the form factor is evaluated and the longitudinal bunch distribution can be retrieved by Fourier inverse transforming Eq.2 as follows

$$g(x) \propto \int_0^\infty \sqrt{F(\omega)}\cos\left(\frac{\omega x}{c}\right) d\omega \tag{9}$$

Since $g(x)$ is real, only the *cos*-term is involved, not allowing to get information on the bunch asymmetry. Furthermore, even assuming non-negative and real electron distribution, an infinite number of different distributions give the same autocorrelation function, since its Fourier transform gives only the absolute magnitude of the form factor, $\left|\sqrt{F(\omega)}\right|$, but no information on the phase. A method, based on Kramers-Kronig dispersion relation and suggested by [3], can be used to retrieve the phase and eliminate the ambiguity in the reconstruction procedure. In principle, for this technique to be completely applicable, the whole frequency spectrum must be known. However, spectral techniques, even though they avoid the synchronization difficulty typical of time domain methods, typically suffer suppressions of the low-frequency part of the spectrum due to diffraction losses from the vacuum pipe and interferometer apertures, together with reduced acceptance and sensitivity of detectors at long wavelengths. Moreover, in case the experimental apparatus is not in vacuum, the transmission of the window as function of the frequency has to be taken into account, resulting in a high-frequency cut-off. Due to this frequency suppression, only a portion of the radiation spectrum is directly measurable, while the low and high part of the spectrum must be extrapolated in order to apply the phase retrieval technique, reducing the accuracy of the bunch profile reconstruction.

The knowledge of the system frequency response, including a precise frequency characterization of detectors, in particular in the millimeter and sub-millimeter range, is mandatory in order to correct the results and extrapolate a bunch shape as close as possible to the real one. The optimum would be the calibration of the detector in the entire frequency spectrum with a unique source. Since this is not straightforward to provide, for the detectors we have studied, i.e. Golay cells, the calibration procedure has been performed by means of three different sources depending on the explored region of the spectrum [4], [5]:

- 4 – 2.7 mm, millimeter wave generator

- 2.1 mm – 1.4 mm – 1.1 mm – 850 μm, hot-cold method with four free-standing mesh filters
- 100 – 160 μm, FEL radiation source.

For all these techniques the goal was the measurement of the detector responsivity, defined as

$$R\left[\frac{V}{W}\right] = \frac{\text{MeasuredVoltageResponse}}{\text{IncidentPower}},$$

as a function of the frequency.
Once the frequency detector response and the transfer function of the whole system are known, the radiation spectrum has to be convoluted with them in order to get the corrected bunch profile.

References

[1] – M. Boscolo et al.
Laser Comb: Simulations of pre-modulated e- Beams at the Photocatode of a High Brightness RF Photoinjector
Proceedings of the 2006 EPAC Conference 98 (2006)
[2] – M. Boscolo et al., NIM A (**577**), 409-416 (2007)
[3] – R. Lai, A.J. Sievers, NIM A (**397**) 221-231 (1997)
[4] – E. Chiadroni, TESLA FEL 2006-9
(http://flash.desy.de/reports_publications/tesla_fel_reports/tesla_fel_2006/index_eng.html)
[5] – H. Delsim-Hashemi et al.,
Detector Response and Beam Line Transmission Measurement with Far-Infrared Radiation
Proceedings of the 27th International Free Electron Laser Conference, Stanford, California (2005)